Nanoscale

PAPER

View Article Online
View Journal | View Issue

Cite this: *Nanoscale*, 2023, **15**, 17956

Ion-induced bias in Ag_2S luminescent nanothermometers†

Marina París Ogáyar, [a] Diego Mendez-Gonzalez, [b,c] Irene Zabala Gutierrez,[c] Álvaro Artiga, [a] Jorge Rubio-Retama,[b,c] Oscar G. Calderón, [d] Sonia Melle, [d] Aida Serrano, [e] Ana Espinosa,[f] Daniel Jaque *[a,b,g,h] and Riccardo Marin *[a,g,h]

Luminescence nanothermometry allows measuring temperature remotely and in a minimally invasive way by using the luminescence signal provided by nanosized materials. This technology has allowed, for example, the determination of intracellular temperature and *in vivo* monitoring of thermal processes in animal models. However, in the biomedical context, this sensing technology is crippled by the presence of bias (cross-sensitivity) that reduces the reliability of the thermal readout. Bias occurs when the impact of environmental conditions different from temperature also modifies the luminescence of the nanothermometers. Several sources that cause loss of reliability have been identified, mostly related to spectral distortions due to interaction between photons and biological tissues. In this work, we unveil an unexpected source of bias induced by metal ions. Specifically, we demonstrate that the reliability of Ag_2S nanothermometers is compromised during the monitoring of photothermal processes produced by iron oxide nanoparticles. The observed bias occurs due to the heat-induced release of iron ions, which interact with the surface of the Ag_2S nanothermometers, enhancing their emission. The results herein reported raise a warning to the community working on luminescence nanothermometry, since they reveal that the possible sources of bias in complex biological environments, rich in molecules and ions, are more numerous than previously expected.

Received 29th July 2023,
Accepted 18th October 2023

DOI: 10.1039/d3nr03728b

rsc.li/nanoscale

1. Introduction

Luminescence nanothermometry makes use of luminescent nanomaterials with temperature-dependent luminescence, which are referred to as luminescent nanothermometers (LNThs).[1] Although LNThs have been successfully used to obtain remote thermal readings in, *e.g.*, miniaturized electronics, it is in the field of biomedicine where the most impressive advances have been made.[2–6] LNThs have been used for diagnosis of tumors,[7,8] diagnosis of affections of the circulatory and nervous systems,[9,10] monitoring of inflammation events and even in studies of single cells.[11–13] Despite the great results and the variety of LNThs reported, luminescence thermometry is being questioned.[14,15] This is because of biases that cast doubts on the reliability of the thermal readouts provided by LNThs.[16]

Biases appear when the luminescence of LNThs – used as signal for achieving a thermal readout – also depends on parameters other than temperature (cross-sensitivity).[17–19] In this situation, changes in the emission spectrum or luminescence decay curves can be erroneously attributed to temperature changes, thus leading to inaccurate thermal readouts. The most frequent source of bias is the induction of spectral distortions caused by changes in the photon extinction by the surrounding medium.[20] There is no "one-size-fits-all" solution to bias, because each combination of LNTh and environment is unique. Thus, to achieve reliable luminescence nanothermometry, effort should be put into understanding the different mechanisms giving rise to biases.

In a recent work, it was demonstrated how bias reduces the reliability of Ag_2S nanoparticles as LNThs during real-time monitoring of a photothermal treatment enabled by magnetic nanoparticles.[21] Therein, bias could not be attributed to

[a]*NanoBIG, Departamento de Física de Materiales, Facultad de Ciencias, Universidad Autónoma de Madrid, C/Francisco Tomás y Valiente 7, Madrid, Spain. E-mail: daniel.jaque@uam.es, riccardo.marin@uam.es*
[b]*Nanobiology Group, Instituto Ramón y Cajal de Investigación Sanitaria (IRYCIS), Ctra. De Colmenar Viejo, Km. 9100, Madrid, Spain*
[c]*Department of Chemistry in Pharmaceutical Sciences, Faculty of Pharmacy, Complutense University of Madrid, Plaza Ramon y Cajal 2, Madrid 28040, Spain*
[d]*Department of Optics, Faculty of Optics and Optometry, Complutense University of Madrid, Arcos de Jalón 118, Madrid E-28037, Spain*
[e]*Instituto de Cerámica y Vidrio | CSIC, Campus de Cantoblanco, C. Kelsen, 5, 28049 Madrid, Spain*
[f]*Instituto de Ciencia de Materiales de Madrid | CSIC, Campus de Cantoblanco, C. Sor Juana Inés de la Cruz, 3, 28049 Madrid, Spain*
[g]*Institute for Advanced Research in Chemical Sciences (IAdChem), Universidad Autónoma de Madrid, Madrid 28049, Spain*
[h]*Instituto Nicolás Cabrera, Universidad Autónoma de Madrid, 28049 Madrid, Spain*
† Electronic supplementary information (ESI) available. See DOI: https://doi.org/10.1039/d3nr03728b

environment-induced spectral distortions and a definitive explanation to the observed lack of reliability in the thermal readout was not given. What is therefore the source of this bias?

In this work, we provide an answer to this question, systematically investigating the performance of Ag_2S LNThs when mixed with magnetic nanoparticles during photothermal processes. The bias mechanism has been identified by combining a series of measurements including (i) study of the impact of the irradiation conditions on the thermal readouts provided by the Ag_2S LNThs, alongside (ii) spectroscopic characterization of the Ag_2S LNThs and (iii) chemical analysis of the dispersant before and after the photothermal procedure. Through these analyses we have uncovered a new bias mechanism involving interaction between Ag_2S LNThs and Fe^{3+} ions. Lastly, we include a critical discussion on the potential impact of this new bias mechanism in luminescence nanothermometry broadly speaking.

2. Results and discussion

2.1. Evidence of bias

The prepared near-infrared (NIR)-emitting Ag_2S LNThs (mean diameter 9 ± 1 nm, HS-PEG-OMe surface coating Fig. S1A†) were first calibrated recording their NIR emission spectrum luminescence in the 20–43 °C temperature range using 0.5 mg mL^{-1} of Ag_2S LNThs in 100 μL of deionized water (Fig. 1A). The behavior is the one expected from the literature:[22,23] a linear decrease in intensity (quenching) is accompanied by a linear red-shift of the peak maximum when increasing the temperature (Fig. 1B).[20,24] The possibility of using multiple thermometric parameters (intensity and peak position) is key in the context of this study, since the thermal readouts obtained with these two parameters are in agreement only if no bias is present.[25]

The Ag_2S LNThs were subsequently mixed in an aqueous dispersion with commercial γ-Fe_2O_3 nanoflowers (NFs; 23 ± 4 nm nominal diameter, dextran-NH_2 surface coating Fig. S1B†) featuring photothermal (PT) properties – meaning that they produce heat under photoexcitation (Fig. 2A), as generally reported for magnetic nanoparticles.[26,27] This mixed dispersion is henceforth referred to as *nanofluid* (Fig. 1SC†). We initially attempted to measure the temperature increase during irradiation of the nanofluid in a 3 × 3 mm^2 cuvette, using a concentration of 0.5 mg mL^{-1} of Ag_2S LNThs and 9.75 mg mL^{-1} of NFs in 100 μL of deionized water. Both Ag_2S LNThs and NFs are known to behave as efficient photothermal transducers. Nevertheless, heating measurements revealed that, under the above concentrations, the heating is mainly generated by NFs (Fig. S2†). The nanofluid was continuously irradiated for 15 min (as a standard for PT treatment) with an 808 nm laser diode (200 mW), while monitoring the temperature with a thermocouple and recording the emission spectrum of the Ag_2S LNThs (Fig. 2B). Two regimes were observed for the Ag_2S LNThs emission during irradiation (Fig. 2C). For the first 3 min, an expected intensity reduction accompanied by a red-shift of the peak maximum was observed due to the heat generated by the NFs. This initial behavior is followed by

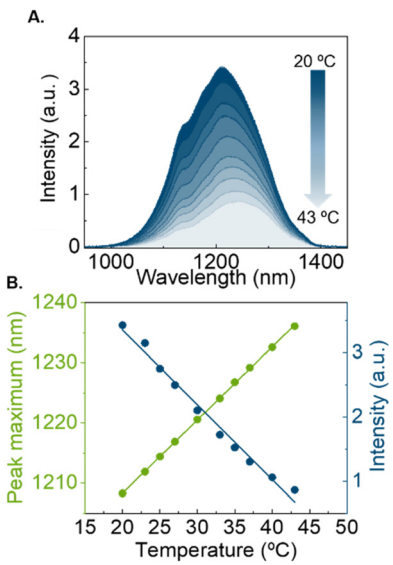

Fig. 1 Characterization of NIR Ag_2S nanoparticles as LNThs. (A) Emission spectra of Ag_2S LNThs obtained at different temperatures (from 20 to 43 °C). (B) Multiparametric thermal readouts of the emission spectra of Ag_2S LNThs. Intensity and shifting of the peak maximum give inverse linear tendencies with Pearson correlation coefficients close to −1 for the emission intensity and 1 for the displacement.

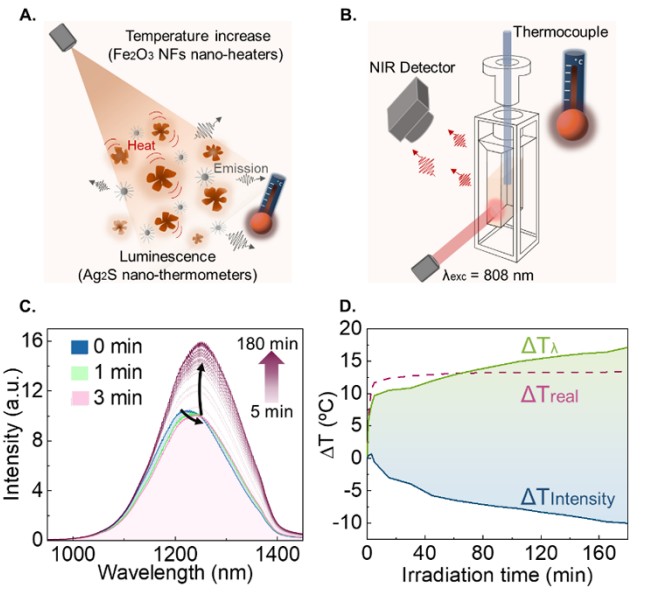

Fig. 2 Characterization of the PT properties of the nanofluid. (A) Representative scheme of the studied nanofluid with heating and temperature-reading properties. Ag_2S LNThs are mixed in dispersion with γ-Fe_2O_3 NFs that have PT properties. (B) Experimental setup. Ag_2S LNThs and magnetic NFs mixture was irradiated with an 808 nm laser diode. The emission spectra were recorded with a NIR detector, and the temperature was measured with a thermocouple. (C) Emission spectra of Ag_2S LNThs in the nanofluid upon laser irradiation. (D) Thermal readouts from thermocouple (ΔT_{real}) and the obtained from Ag_2S LNThs, intensity ($\Delta T_{intensity}$) and peak maximum shift (ΔT_{λ}).

an increase of intensity to 153% of the initial value after 3 h of irradiation. Note that while the irradiation time was extended up to 3 h to properly study the observed phenomenon, after a few minutes into the PT treatment the intensity enhancement was already noticeable. This intensity increment goes hand in hand with a counterintuitive red-shift of the peak position. These two observations do not seem to be reconcilable, since they would correspond to diametrically opposite thermal readouts: a temperature decrease according to the intensity variation and a temperature increase according to the shift in peak position (Fig. 2D). The thermocouple reading is in fairly good agreement – although with significant discrepancies in slopes and measured temperature increase – with the temperature increase obtained from the analysis of the peak shift (Fig. 2D). A difference in temperature is partially expected between the thermocouple readout and the one given by Ag_2S LNThs due to heat dissipation through water and the macroscopic average readout achieved with the thermocouple.[28] The opposite behavior shown by the readouts obtained through the two luminescence thermometry parameters points to a clear bias in the Ag_2S LNThs thermometric performance upon mixing them with NFs (compare Fig. 1A and 2C). The origin of this bias is explored in the next section.

2.2. Identification of the mechanism inducing bias

Aside from spectral information, we decided to also explore the photoluminescence dynamics of the system, since it brings additional insight into the changes occurring in the emitting species. Specifically, we recorded photoluminescence decay curves for the Ag_2S LNThs in the nanofluid before and after irradiation, using a concentration of 0.5 mg mL^{-1} of Ag_2S LNThs and 9.75 mg mL^{-1} of NFs in 100 μL of deionized water (Fig. 3A). Upon irradiation, the average lifetime increased by 100% (from 216 to 428 ns). These results suggest a structural or compositional change at the surface or within the volume of the Ag_2S LNThs, which are mirrored by changes in the electronic structure of the emitters. Indeed, it is widely reported that the nonradiative decay of Ag_2S nanoparticles can be reduced simply altering the chemical composition of their surface.[29–32] To better understand the processes involved, we systematically investigated the impact that different parameters have on the observed intensity enhancement:

- *Effect of NF concentration.* We monitored the enhancement in the Ag_2S LNThs emitted intensity during PT processes for different NF concentrations (Fig. 3B). In the absence of NFs, a 30% intensity decrease was observed, revealing a local thermal increment of approximately 10 °C. Once the NFs are incorporated, the Ag_2S LNThs start failing to provide indications of laser induced heating: instead of an intensity quenching (indicating heating) an intensity enhancement was observed. The magnitude of the intensity enhancement is proportional to the NFs concentration, with up to a 4-fold increase at the highest studied NF concentration (9.5 mg mL^{-1}; corresponding to 3

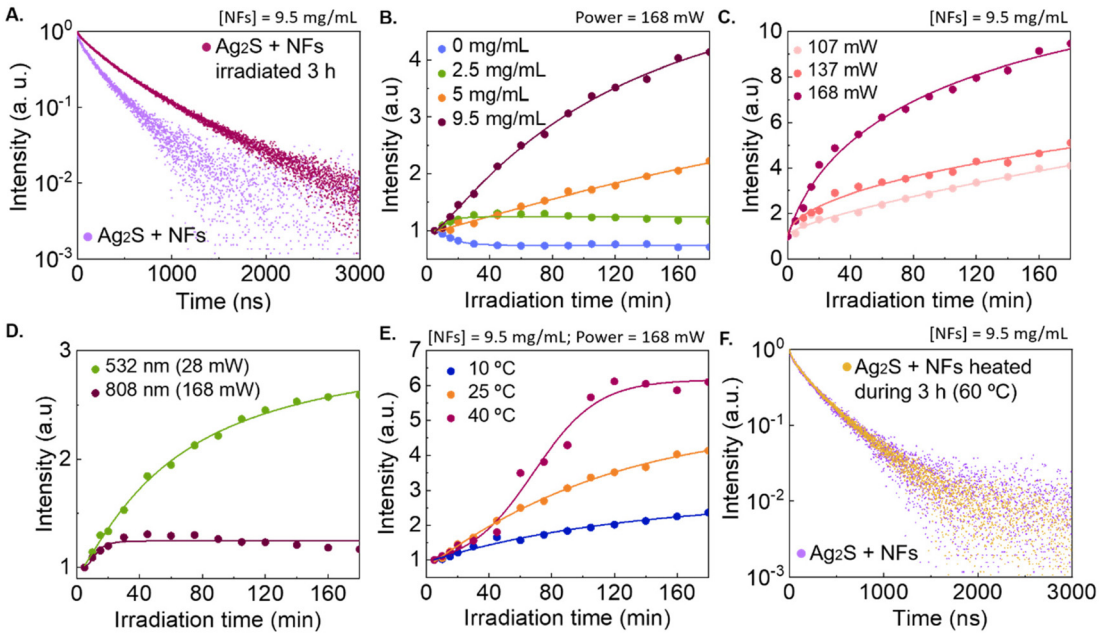

Fig. 3 Characterization of the changes in the properties of Ag_2S LNThs in the presence of NFs. (A) Photoluminescence decay curves of Ag_2S LNThs in the nanofluid before and after irradiating for 3 h (808 nm laser diode, 200 mW). (B) Enhancement of the emission intensity of Ag_2S LNThs (0.5 mg mL^{-1}) upon irradiation at various NF concentrations (0, 2.5, 5 and 9.5 mg mL^{-1}). (C) Enhancement of the emission intensity of Ag_2S LNThs (0.5 mg mL^{-1}) varying the power of the excitation laser (107, 137 and 168 mW) and maintaining the NF concentration at 9.5 mg mL^{-1}. (D) Enhancement of the emission intensity of Ag_2S LNThs (0.5 mg mL^{-1}) changing the laser excitation wavelength: 532 nm (28 mW) using 2.5 mg mL^{-1} of NFs and 808 nm (168 mW) using 9.5 mg mL^{-1} of NFs. (E) Enhancement of the emission intensity of Ag_2S LNThs in the presence of NFs (9.5 mg mL^{-1}) upon irradiation at 808 nm, varying the temperature of the dispersing medium (10, 25, and 40 °C). (F) Normalized photoluminescence decay curves obtained before and after heating the nanofluid to 60 °C for 3 h (measurements performed both at room temperature).

Ag_2S LNThs per NF). These results highlight the presence of an interaction between Ag_2S LNThs and NFs that is more relevant as the concentration of the NFs increases.

- *Effect of laser power and wavelength.* Upon fixing the NF concentration to 9.5 mg mL^{-1}, we studied the effect of the 808 nm laser power (Fig. 3C), observing that higher powers correspond to a greater emission intensity enhancement and a faster rate of change. For example, a power of 107 and 168 mW leads to a 260 and 860% enhancement, respectively. Furthermore, we decided to investigate the effect of using an irradiation wavelength more efficiently absorbed by the NFs (Fig. S3†).[33,34] Under 532 nm irradiation with laser power of 28 mW (Fig. 3D), a greater enhancement is observed compared to the one obtained using a 808 nm laser and a power of 168 mW (20 *vs.* 160%). The higher photon absorption at 532 nm also forced us to bring down the NF concentration to 2.5 mg mL^{-1}, so that the emission of the Ag_2S LNThs could be properly monitored (*i.e.*, more excitation photons could reach the Ag_2S LNThs). This difference in NF concentration between the experiments conducted with the 532 and 808 nm lasers makes the results even more staggering. Both the excitation with a higher laser power and the use of a wavelength more efficiently absorbed by the NFs lead to higher local temperatures (due to the PT effect described previously). We thus decided to specifically investigate the effect of this parameter.

- *Effect of the nanofluid temperature.* For this set of experiments, the temperature of the nanofluid was externally set to 10, 25, and 45 °C, observing that the degree of emission intensity enhancement is higher for higher temperatures (Fig. 3E). These results are well in agreement with the above observations that highlight how temperature plays a role in the process.

Altogether, these results point towards an enhancement of the Ag_2S LNTh emission intensity (and lifetime lengthening) driven by a photo-induced interaction with the NFs, which is accelerated at higher temperatures. Additionally, we confirmed that the effect does not occurr by simply heating the nanofluid for 3 h (Fig. 3F), suggesting that localized heating at the nanoparticle level is required for the effect to be noticeable.

These observations allowed us to narrow down our search to two possible sources of changes in spectroscopic properties of the Ag_2S LNThs and hence, the presence of bias: a photo-induced release of $Fe^{2+/3+}$ ions or a photocatalytic effect. The following experiments were thus conducted to identify the source of the bias.

- *Iron ion release.* Iron oxide nanoparticles in aqueous media are known to release a small amount of $Fe^{2+/3+}$ ions over time.[35] We thus postulated that the NFs used in this study would be induced to release $Fe^{2+/3+}$ ions at faster rates during laser irradiation due to the local heating. To verify this, we used a colorimetric assay (Fig. 4A and Fig. S4A†) to identify the presence of free iron ions in the medium before and after irradiation of a 9.5 mg mL^{-1} dispersion of NFs (no Ag_2S LNThs were added at this stage). The assay relies on the use of 1,10-Phenanthroline as chelating agent. This molecule forms a strongly colored orange-red metal complex in the presence of

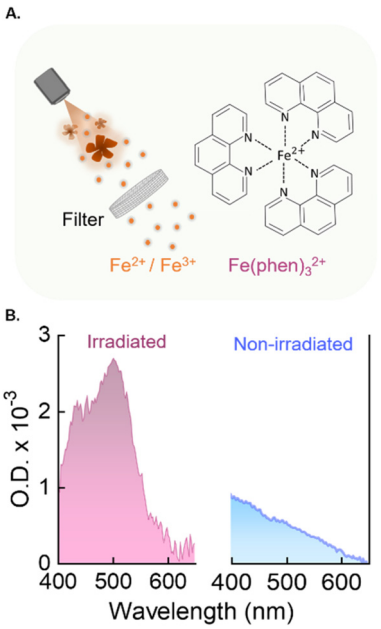

Fig. 4 Detection of iron ions. (A) Scheme of the purification process and the metal complex used for detecting the presence of released iron ions. Irradiated NFs (or non-irradiated for control) were filtered, and the filtrate was treated with 1,10-Phenanthroline (phen), resulting in the orange-red metal complex $[Fe(phen)_3]^{2+}$. (B) Extinction spectra obtained from the filtrates of NF dispersions without (blue) and with (magenta) 808 nm irradiation (P = 200 mW).

Fe^{2+}, which can be detected *via* absorption spectrophotometry. To account for all free iron ions, after removing the NFs *via* centrifugation, the medium was treated with an hydroxylamine solution to reduce possible Fe^{3+} ions to Fe^{2+}.[36] The results of these tests prove that a measurable amount of iron is released only when the NFs are irradiated (Fig. 4B). Upon extrapolating the values of the calibration curve, we estimated that the irradiation led to a release of iron amounting to a final concentration of 2 μM (see ESI Fig. S4B and 4SC†).

- *Photocatalytic effects.* We also evaluated the possible production of reactive oxygen species (ROS) by NFs during 808 nm irradiation by monitoring the degradation of Rhodamine B (RhB) under irradiation.[37] Comparing the results obtained irradiating with a 808-nm laser an RhB solution (12.25 μM) in the presence or absence of NFs, we could not observe significant differences in the decomposition of RhB (Fig. S5A and S5B†). Therefore, we concluded that if ROS were generated during the irradiation, these were not in high enough quantity to substantially contribute to the observed changes in the spectroscopic properties of the Ag_2S LNThs.

To unequivocally verify that the released iron ions are responsible for the change in the spectroscopic features of Ag_2S LNThs (note that no change in the pH value was observed during the experiments), we compared the emission spectrum and photoluminescence decay curves of an Ag_2S LNThs dispersion before and after addition of Fe^{3+} ions.

Upon adding 2 μL of 1 mM $FeCl_3$ to 98 μL 0.5 mg mL^{-1} Ag_2S LNThs dispersion (approximately 20 μM of Fe^{3+} in the

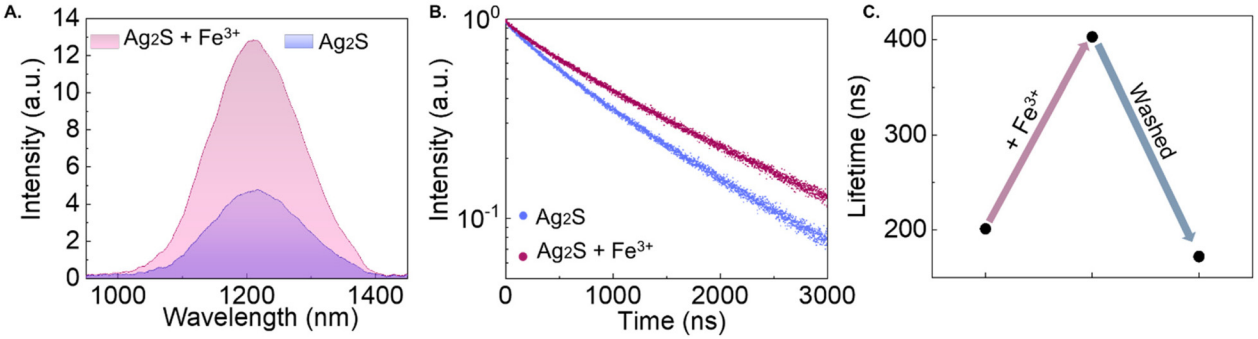

Fig. 5 Effect of iron ions. (A) Emission spectra measured at 20 °C of Ag_2S LNThs as synthesized and upon 2 μL of 1 mM $FeCl_3$ addition. (B) Lifetime measurements measured at 20 °C of Ag_2S LNThs as synthesized and upon 2 μL of 1 mM $FeCl_3$ addition. (C) Lifetime values measured at 20 °C of Ag_2S LNThs as synthesized, upon 2 μL of 1 mM $FeCl_3$ addition and after washing.

final solution), an enhancement in the emission intensity (280%, Fig. 5A) and a lengthening of the lifetime (30%, Fig. 5B) was observed. We should also point out that a different Ag_2S LNThs batch was used for these experiments. As such, the discrepancies in the absolute values of lifetime and relative changes observed compared to the results showed in Fig. 3 are to be ascribed to interbatch variabilities. Although there is also the possibility that other parameters are contributing to the changes in the optical properties of Ag_2S LNThs, such as local temperature increases. The confirmation that these changes are induced by surface modifications was obtained from observation of the reversibility of the effect. Indeed, after washing the Ag_2S LNThs *via* centrifugation after the addition of the $FeCl_3$ solution, the lifetime values were recovered (Fig. 5C). This result suggests that iron ions did not diffuse into the crystal structure of the Ag_2S LNThs but rather remained weakly tethered to their surface, possibly due to the lack of ligands in the solution supporting incorporation by cation exchange.[38]

It should be noted that the concentration of Fe^{3+} ions added in this test is 10 times higher than the one estimated during the irradiation (Fig. 4 and Fig. S4†). This is because no significant changes in the spectral properties were detectable using a concentration of 2 μM. This discrepancy could be explained considering that the concentration obtained using the colorimetric assay is an underestimation, since part of the $Fe^{2+/3+}$ ions released under irradiation could be retained at the surface of the NFs by NH_2 (present in the amino-dextran coating of the NFs). Moreover, a concentration of iron ions of approximately 20 μM is on par with the serum free iron concentration found in human body.[39]

The involvement of the surface rather than the bulk of Ag_2S LNThs in this process is also supported by comparison of our results with the ones reported in the literature. Previous studies show that intentional incorporation of ions like Au^{3+} and Pb^{2+} in the lattice leads to an increased emission efficiency of silver chalcogenide nanocrystals, which is also accompanied by a shift of the emission peak.[29,40–42] The absence of relevant incorporation of iron ions into the volume of Ag_2S LNThs is supported by the absence of such shift in the emission peak position (Fig. 5A).

We also attempted to get direct evidence of the presence of iron attached to the Ag_2S LNThs, performing elemental mapping of the nanofluid after irradiation (Fig. S6†). Yet, this analysis was not conclusive probably due to the low concentration of the released ions during the irradiation process. Lastly, the possible presence of contribution of partial oxidation and incorporation of iron into the Ag_2S LNThs was also studied with X-ray absorption spectroscopy (XAS) (Fig. S7A†) measurements at the Ag K-edge (25 514 eV) performed at the BM30 beamline (ESRF synchrotron, Grenoble, France). A change in valence (to be expected in the case of oxidation) was discarded by extended X-ray absorption fine structure (EXAFS) (Fig. S7B and S7C†). At larger interatomic distances, a variation in the position and the intensity is detected in the irradiated sample. The observed changes could be related to the incorporation of Fe in the structure. Therefore, changes in the surface chemistry of the Ag_2S LNThs are to be considered the main responsible for the observed variations in their spectroscopic properties.

2.3. Ion-induced bias: a broader issue in luminescence nanothermometry?

We have shown how mixing Ag_2S and γ-Fe_2O_3 nanoparticles leads to changes in the optical properties of the luminescent species used as LNThs under irradiation, and hence to a faulty thermal readout. The effect reported herein indicates that the thermal readout capability of the LNThs is somehow retained using one thermometric parameter (spectral shift), while the other parameter (absolute intensity) becomes completely unreliable. The case study herein reported is admittedly a specific one, but the processes involved are general in nature.

In fact, LNThs are supposed to work in complex biological environments, where several ions are naturally present: some in higher, other in lower concentrations. The most abundant metal ions constituting the human body include alkali and alkaline earth ions like Na^+, K^+, Ca^{2+} and Mg^{2+}. These metal ions are crucial for many functions in our body such as neuro-

transmission or blood circulation,[43] and are present at concentrations up to 10^2 mM.[44] Other oligo-element metals (*i.e.* trace elements that are found in smaller quantities in the body but are necessary for humans)[45] include $Fe^{2+/3+}$, Cu^{2+}, Zn^{2+}, and Mn^{2+}.[46] Among the different transition metal, iron is the most prevalent one in the body, in both oxidation states $Fe^{2+/3+}$,[43] with serum free iron concentration in concentrations between 10–30 μM.[39] When LNThs (but any nanoparticle, really) are introduced in the human body, they are therefore bound to interact with these ions. In addition, local variations in the ionic strength and in temperature in living organisms are to be expected and external irradiation might lead to further localized heating. These temperature changes might promote mechanisms like cation exchange between ions already present in solution and the LNThs. Heat-promoted incorporation of ions has been reported in semiconductor nanocrystals as well as in lanthanide-doped nanoparticles (the two classes of luminescent nanoparticles used the most in luminescence nanothermometry), and the associated changes in optical properties are sizeable.[38,47–49] Therefore, we claim that, in the evaluation of the reliability of a luminescence nanothermometry approach, care should be taken in considering possible ion-induced effects beyond the ones merely induced by the ionic strength of the medium. As a last remark, we would like to highlight that strategies like coating with suitable polymeric and inorganic shells may prove useful to avoid detrimental effects such as the one discussed previously. Efforts in this direction are expected to contribute solving the issue of frequent lack of reliability of luminescence nanothermometry in complex biological media.

3. Conclusions

In this study, we showed that the performance of Ag_2S luminescent nanothermometers (LNThs) can be affected by a previously overseen source of bias: the interaction of the LNThs with metal ions in solution. We discovered this effect by investigating the possibility of measuring the magnitude of temperature increase during photothermal (PT) processes in a nanofluid composed of Ag_2S LNThs and iron oxide nanoflowers (NFs). Specifically, during the irradiation with a near infrared laser (808 nm), the Ag_2S LNThs in the nanofluid exhibited an unexpected enhancement of emission intensity instead of the expected heating-induced luminescence quenching. We verified that the enhancement in emission intensity depends on the NF concentration, the temperature of the nanofluid, as well as the power and wavelength of the laser. With the help of a colorimetric assay, a release of iron ions from the NFs under irradiation was observed. These ions appear to be weakly bound to the surface of the Ag_2S LNThs, modifying their luminescent properties. As such, the Ag_2S LNThs cease to be reliable luminescent nanothermometers.

This work therefore raises an important caveat: the interaction between LNThs and free ions in the medium could affect the reliability of the thermometric approach. These interactions could be especially significant when working in biological media since different ions are naturally present. Such observations reinforce the need for a thorough understanding of how the LNThs can interact with complex media (particularly in the biological context) to achieve a reliable thermal readout.

Conflicts of interest

There are no conflicts to declare.

Acknowledgements

This work was financed by the Spanish Ministerio de Ciencia e Innovación under project NANONERV PID2019-106211RB-I00. R. M. is grateful to the Spanish Ministerio de Ciencia e Innovación for support to research through a Ramón y Cajal Fellowship (RYC2021-032913-I). M. P. acknowledges the financial support from the Spanish Ministerio de Ciencia e Innovación for a FPU (FPU20/03166). A. S. and A. E. acknowledge the MICIN for the financial support from Ramón y Cajal program (RYC2021-031236-I funded by the Recovery, Transformation and Resilience plan and RYC2020-029282-I, respectively). A. A. is grateful to the Spanish Ministerio de Ciencia e Innovación for financial support through a Juan de la Cierva Fellowship (FJC2021-047006-I). We also thank the BM30 beamline staff at ESRF synchrotron for their technical support.

References

1 D. Jaque and F. J. N. Vetrone, *Nanoscale*, 2012, **4**, 4301–4326.
2 M. Runowski, P. Woźny, N. Stopikowska, I. R. Martín, V. Lavín and S. Lis, *ACS Appl. Mater. Interfaces*, 2020, **12**, 43933–43941.
3 R. G. Geitenbeek, A.-E. Nieuwelink, T. S. Jacobs, B. B. Salzmann, J. Goetze, A. Meijerink and B. M. Weckhuysen, *ACS Catal.*, 2018, **8**, 2397–2401.
4 J. Drabik, R. Kowalski and L. Marciniak, *Sci. Rep.*, 2020, **10**, 11190.
5 A. Bednarkiewicz, L. Marciniak, L. D. Carlos and D. Jaque, *Nanoscale*, 2020, **12**, 14405–14421.
6 I. V. Barbosa, L. J. Maia, A. Ibanez and G. Dantelle, *Opt. Mater.: X*, 2023, 100236.
7 H. D. Santos, E. C. Ximendes, M. d. C. Iglesias-de la Cruz, I. Chaves-Coira, B. del Rosal, C. Jacinto, L. Monge, I. Rubia-Rodríguez, D. Ortega and S. Mateos, *Adv. Funct. Mater.*, 2018, **28**, 1803924.
8 Q. Fan, C. Sun, B. Hu and Q. Wang, *Mater. Today Bio*, 2023, 100646.
9 E. C. Ximendes, U. Rocha, B. Del Rosal, A. Vaquero, F. Sanz-Rodríguez, L. Monge, F. Ren, F. Vetrone, D. Ma and J. García-Solé, *Adv. Healthcare Mater.*, 2017, **6**, 1601195.

10 P. Rodríguez-Sevilla, R. Marin, E. Ximendes, B. Del Rosal, A. Benayas and D. Jaque, *Front. Chem.*, 2022, **10**, 941861.
11 Y. Shen, J. Lifante, I. Zabala-Gutierrez, M. de la Fuente-Fernández, M. Granado, N. Fernández, J. Rubio-Retama, D. Jaque, R. Marin and E. Ximendes, *Adv. Mater.*, 2022, **34**, 2107764.
12 M. Garvas, S. Acosta, I. Urbančič, T. Koklič, J. Štrancar, L. A. Nunes, P. Guttmann, P. Umek and C. Bittencourt, *Nano Sel.*, 2021, **2**, 1208–1217.
13 H. Liu, Y. Fan, J. Wang, Z. Song, H. Shi, R. Han, Y. Sha and Y. Jiang, *Sci. Rep.*, 2015, **5**, 14879.
14 L. Labrador-Paez, M. Pedroni, A. Speghini, J. Garcia-Sole, P. Haro-Gonzalez and D. Jaque, *Nanoscale*, 2018, **10**, 22319–22328.
15 J. C. Martins, A. R. Bastos, R. A. Ferreira, X. Wang, G. Chen and L. D. Carlos, *Adv. Photonics Res.*, 2021, **2**, 2000169.
16 Y. Shen, J. Lifante, N. Fernandez, D. Jaque and E. Ximendes, *ACS Nano*, 2020, **14**, 4122–4133.
17 P. Rodríguez-Sevilla, G. Spicer, A. Sagrera, A. P. Adam, A. Efeyan, D. Jaque and S. A. Thompson, *Adv. Opt. Mater.*, 2023, 2201664.
18 A. D. Pickel, A. Teitelboim, E. M. Chan, N. J. Borys, P. J. Schuck and C. Dames, *Nat. Commun.*, 2018, **9**, 4907.
19 M. Suta, Ž. Antić, V. Đorđević, S. Kuzman, M. D. Dramićanin and A. Meijerink, *Nanomaterials*, 2020, **10**, 543.
20 J. Zhou, B. Del Rosal, D. Jaque, S. Uchiyama and D. Jin, *Nat. Methods*, 2020, **17**, 967–980.
21 D. Mendez-Gonzalez, J. Lifante, I. Z. Gutierrez, R. Marin, E. Ximendes, E. Sanz-de Diego, M. C. Iglesias-de la Cruz, F. J. Teran, J. Rubio-Retama and D. Jaque, *Nanoscale*, 2022, **14**, 16208–16219.
22 R. Marin, A. Benayas, N. García-Carillo, J. Lifante, J. Yao, D. Mendez-Gonzalez, F. Sanz-Rodríguez, J. Rubio-Retama, L. V. Besteiro and D. Jaque, *Adv. Photonics Res.*, 2022, **3**, 2100260.
23 Y. Shen, J. Lifante, E. Ximendes, H. D. Santos, D. Ruiz, B. H. Juárez, I. Z. Gutiérrez, V. T. Vera, J. R. Retama and E. M. Rodríguez, *Nanoscale*, 2019, **11**, 19251–19264.
24 Y. Shen, H. D. Santos, E. C. Ximendes, J. Lifante, A. Sanz-Portilla, L. Monge, N. Fernandez, I. Chaves-Coira, C. Jacinto and C. D. Brites, *Adv. Funct. Mater.*, 2020, **30**(49), 2002730.
25 T. A. Alrebdi, A. N. Alodhayb, Z. Ristić and M. D. Dramićanin, *Sensors*, 2023, **23**, 3839.
26 S. Shaw, J. Kailashiya, A. Gangwar, S. Alla, S. K. Gupta, C. Prajapat, S. S. Meena, D. Dash, P. h. Maiti and N. Prasad, *Appl. Surf. Sci.*, 2021, **560**, 150025.
27 A. Espinosa, R. Di Corato, J. Kolosnjaj-Tabi, P. Flaud, T. Pellegrino and C. Wilhelm, *ACS Nano*, 2016, **10**, 2436–2446.
28 E. Glais, A. Maître, B. Viana and C. Chanéac, *Nanoscale Adv.*, 2021, **3**, 2862–2869.
29 H. Yang, R. Li, Y. Zhang, M. Yu, Z. Wang, X. Liu, W. You, D. Tu, Z. Sun and R. Zhang, *J. Am. Chem. Soc.*, 2021, **143**, 2601–2607.
30 Z. Wang, T. Gu, T. Kadohira, T. Tada and S. Watanabe, *J. Chem. Phys.*, 2008, **128**(1), 014704.
31 M. Hamilton, A. Barnes, W. Howells and H. Fischer, *J. Phys.: Condens. Matter*, 2001, **13**, 2425.
32 H. D. Santos, I. Zabala Gutiérrez, Y. Shen, J. Lifante, E. Ximendes, M. Laurenti, D. Méndez-González, S. Melle, O. G. Calderón and E. López Cabarcos, *Nat. Commun.*, 2020, **11**, 2933.
33 J. R. Albani, Chapter 2-Fluorescence: Principles and Observables, in *Structure and Dynamics of Macromolecules: Absorption and Fluorescence Studies*, Elsevier Science, 2004, pp. 55–98.
34 M. A. Omary and H. H. Patterson, in *Encyclopedia of Spectroscopy and Spectrometry*, ed. J. C. Lindon, G. E. Tranter and D. W. Koppenaal, Academic Press, Oxford, 3rd edn, 2017, pp. 636–653.
35 L. Voss, E. Hoché, V. Stock, L. Böhmert, A. Braeuning, A. F. Thünemann and H. Sieg, *Arch. Toxicol.*, 2021, **95**, 895–905.
36 E. Agustina, J. Goak, S. Lee, Y. Seo, J. Y. Park and N. Lee, *ChemistryOpen*, 2015, **4**, 613–619.
37 P. Van Viet, D. Van Chuyen, N. Q. Hien, N. N. Duy and C. M. Thi, *J. Sci.: Adv. Mater. Devices*, 2020, **5**, 308–315.
38 L. De Trizio and L. Manna, *Chem. Rev.*, 2016, **116**, 10852–10887.
39 P. Bennett, C. Williamson, L. Sykes, D. A. MacIntyre and P. H. Dixon, *Basic Science in Obstetrics and Gynaecology E-Book: A Textbook for MRCOG Part 1*, Elsevier Health Sciences, 2022.
40 Y. Shu, J. Yan, Q. Lu, Z. Ji, D. Jin, Q. Xu and X. Hu, *Sens. Actuators, B*, 2020, **307**, 127593.
41 M. Yu, X. Yang, Y. Zhang, H. Yang, H. Huang, Z. Wang, J. Dong, R. Zhang, Z. Sun and C. Li, *Small*, 2021, **17**, 2006111.
42 H. Yang, H. Huang, X. Ma, Y. Zhang, X. Yang, M. Yu, Z. Sun, C. Li, F. Wu and Q. Wang, *Adv. Mater.*, 2021, **33**, 2103953.
43 X. Zheng, W. Cheng, C. Ji, J. Zhang and M. Yin, *Rev. Anal. Chem.*, 2020, **39**, 231–246.
44 A. Melkikh and M. Sutormina, *J. Theor. Biol.*, 2008, **252**, 247–254.
45 D. C. Carvalho, L. M. Coelho, M. S. M. Acevedo and N. M. Coelho, *Handbook of mineral elements in food*, 2015, pp. 109–122.
46 N. P. Zaksas, S. E. Soboleva and G. A. Nevinsky, *Sci. World J.*, 2019, **1**, 1–9.
47 L. Jin, J. Liu, X. Liu, D. Benetti, G. S. Selopal, X. Tong, E. Hamzehpoor, F. Li, D. F. Perepichka and Z. M. Wang, *Small Methods*, 2023, 2300133.
48 C. Dong and F. C. van Veggel, *ACS Nano*, 2009, **3**, 123–130.
49 L. Labrador-Páez, M. Pedroni, K. Smits, A. Speghini, F. Jaque, J. García-Solé, D. Jaque and P. Haro-González, *Part. Part. Syst. Charact.*, 2017, **34**, 1700276.